# Scientific Visualization and Application of Massively Parallel Computing Techniques in the Design and Analysis of Optimized Low Aspect Ratio Stellarators

D. A. Spong, S. P. Hirshman, D. B. Batchelor, L. A. Berry,
J. Carlsson, J. F. Lyon, R. Sanchez, J. C. Whitson
Oak Ridge National Laboratory
Oak Ridge, TN 37831-8071

**I. <u>Introduction</u> -** There has been a resurgence of interest in stellarator physics and design in the U. S. fusion program in recent years. This has been facilitated by the development of improved optimization strategies that offer the promise of compactness (low aspect ratio) while retaining good confinement and stability properties.[1,2,3,4] Compactness is desireable both for near-term devices where it offers larger plasma size at fixed cost and for reactors where it allows lower cost for a fixed amount of fusion power. We have developed an optimization method[1-3] which successfully integrates a wide range of physics criteria into the design process for such devices. The flexibility offered by 3-dimensional shaping of the outer flux surface has allowed new drift-optimized compact configurations with plasma aspect ratios $A_p = \langle R\rangle/\langle a\rangle = 2 - 4$ to be developed which can combine some of the best features of tokamaks (moderate aspect ratio, good confinement and beta) and stellarators (disruption immunity, no current drive, low recirculating power in a reactor). The optimization approach described here, known as quasi-omnigeneity or J*-symmetry (J* is the approximate second adiabatic invariant), initially[1,2] focused on confinement improvement through minimizing the deviation of the bounce-averaged trapped particle drift orbits from magnetic flux surfaces. As this approach has evolved, an increasing array of physics objectives have been added, including Mercier and ballooning stability, bootstrap current consistency, specified rotational transform profiles (i.e., so as to avoid major resonances and neoclassical MHD tearing modes), and various measures of magnetic coil complexity. This effort has resulted in a device, QOS, which will be proposed for a modest ($\langle R\rangle \sim 1$ meter, $\langle B\rangle \sim 1$ Tesla, $P_H < 2$Mw) concept exploration experiment designed to test the confinement and flexibility of this approach. In addition to good confinement at low aspect ratio, some of the unique features this device offers are: (a) low levels of bootstrap current, (b) moderately high rotational transform ($\iota$ in the range of 0.5 to 0.8), and (c) equilibria which are relatively insensitive to changes in $\langle\beta\rangle$. In the following we shall discuss the methods used for obtaining QO stellarators, and the physics tools used to analyze their performance; scientific visualization[5] and high performance computing have significantly facilitated this effort.

**II. <u>Stellarator Optimization Method</u> -** The general goals of our near-term experiment design effort are: (a) energy confinement times $\tau_E > 2\tau_{E,ISS95}$ , where $\tau_{E,ISS95}$ is the empirical stellarator confinement scaling[6]; (b) $\langle\beta\rangle \sim 4\%$ (for a reactor); and (c) modular coils with sufficient access for heating and diagnostics. Our optimization procedure varies the outer magnetic flux surface shape (described by 30-40 Fourier harmonics for $R_{mn}$ and $z_{mn}$), plasma current, and pressure profiles to minimize a set of physics and engineering target functions. This is accomplished in an automated way

by using the VMEC equilibrium code within a Levenberg-Marquardt optimization loop. Human intervention is required in selecting the initial configuration, the weights applied to the target functions and the form of the target functions (see table below). Not all of these targets are necessarily applied simultaneously (e.g., iota profile vs. current profile and maximum current).

| **Targets** | **Example** |
|---|---|
| Bounce-average omnigeneity (drift surfaces and flux surfaces aligned) | $B_{min} = B_{min}(\psi)$<br>$B_{max} = B_{max}(\psi)$<br>$J^* = J^*(\psi)$ |
| Current profile | monotone increasing $I(\psi)$<br>self-consistent $I_{BS}$ |
| Limit maximum plasma current | e.g., $I_{max} < 40$ kAmps |
| Iota profile | $i(\rho) = 0.5$ ($\rho$=0) to 0.8 ($\rho$=a) avoid major resonances |
| Magnetic Well, Mercier | $V'' < 0$, $D_M > 0$ over cross section |
| Ballooning stability | Stable up to $\langle\beta\rangle \sim 4\%$ |
| Aspect ratio | $R_0/a \approx 3$ to 4 |
| Limit outer surface curvature | avoid strong elongation/cusps |

These target functions are continuously being augmented and refined. In the near future we anticipate: (a) replacing the J* target function with a measure more representative of the exact J invariant, (b) utilizing the DKES code to develop a diffusive transport target, and (c) introducing measures of energetic particle confinement (possibly particle based) into the optimization loop.

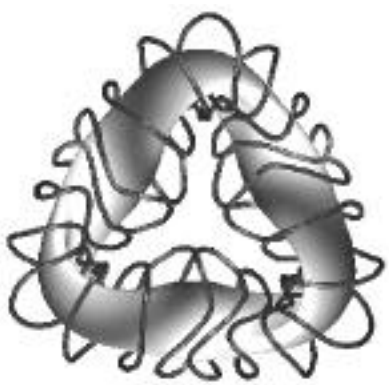

Figure 1 – Coils and outer flux surface shape of a three field period QOS device.

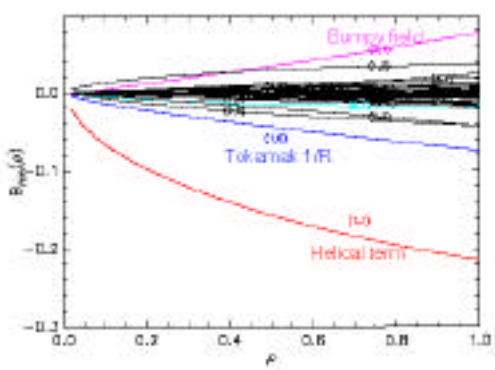


Figure 2 – $B_{mn}$ spectrum vs. flux surface for this device.

Coil geometries which produce the outer surface shapes generated by the physics targets are arrived at by a second optimization loop which varies coil shapes in order to minimize the normal component of magnetic field on the outer surface. One of our typical three-field period configurations with coils is shown in Fig. 1 along with its magnetic field spectrum. As may be seen, the magnetic field spectrum is dominated by the helical component, but not to the extent that would be the case for a quasi-helical device. This device then represents something of a hybrid between the W7-X device[7] (where the bumpy component is more dominant) and a quasi-helical device such as HSX[8]; although it is at a significantly lower aspect ratio (A = <R>/<a> = 3 - 4) than either W7-X or HSX. The finite spread of the lower amplitude modes in Fig. 2 can represent a source of design flexibility; small variations in these components can allow improvements in ballooning stability and better tailoring of the bootstrap current profile.

An example of stability optimization using the recently introduced COBRA[9] rapid ballooning analysis algorithm is shown in Figs. 3 and 4 where an initially unstable configuration was made stable up to <β> = 3% using moderate shape changes in the surfaces. Further stabilization up to <β> = 4% was then accomplished through small pressure profile changes.

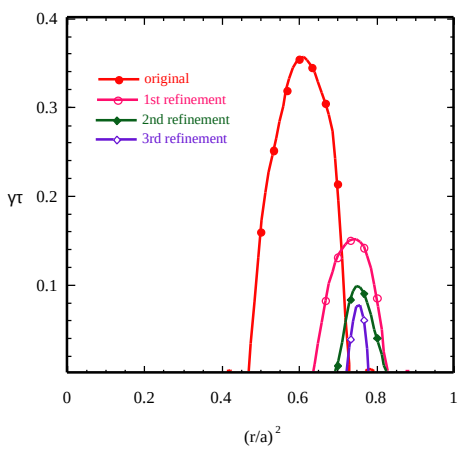


Figure 3 – Decreasing ballooning instability growth rates with successive optimization.

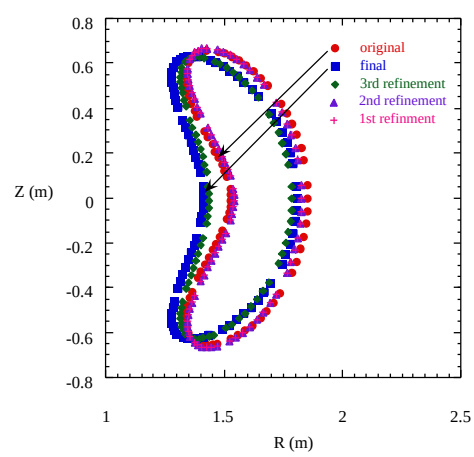


Figure 4 – Flux surface changes (shown at ζ = 0°) which lead to these growth rate changes.

Another recent improvement in our set of optimization targets is the inclusion of a self-consistent bootstrap current. This is calculated in the collisionless limit and the difference between the assumed VMEC plasma current and the predicted bootstrap current is minimized. Our bootstrap current is in the opposite direction to that of the equivalent axisymmetric device (i.e., it reduces transform). We expect, in the near future to examine devices with small levels of positive bootstrap current (i.e., in the additive direction). The typical degree of bootstrap current alignment and its modification of the rotational transform profile are shown below in Figures 5 and 6.

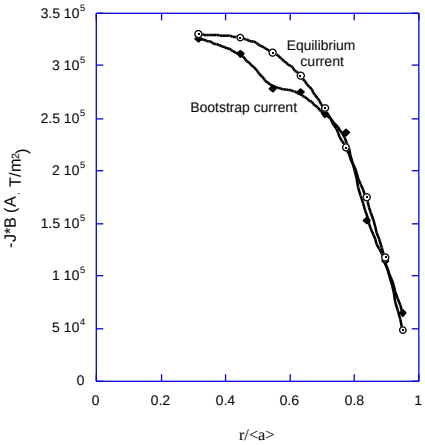


Figure 5 – Collisionless bootstrap current profile and VMEC current profile for three-period QOS device.

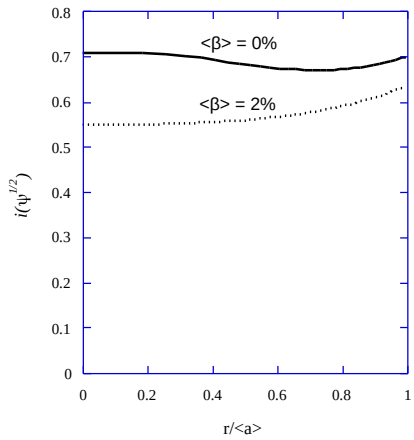


Figure 6 – Self-consistent rotational transform profiles at <β> = 0 and 2%.

**III. <u>Physics Studies of Optimized Configurations</u> -** We have developed several tools for more in-depth analysis of the confinement and stability of our configurations outside of the optimization loop described above. As mentioned earlier, the COBRA code is used to examine high-n ballooning stability. Also, external kink stability been analyzed in a few cases; although the low plasma currents predicted for near-term QO devices are not expected to be a strong drive for kinks, further work needs to be done in this area. Confinement analysis is carried out both using particle-based Monte Carlo methods as well as continuum solutions of the Fokker-Planck equation provided by the DKES[10] code.

These particle calculations are done with the DELTA5D code run in parallel on the Cray T3E using the MPI language for communication between processors; a near linear speed-up with the number of processors is observed. This code currently has options in it for several classes of energetic particle populations, including fusion-produced alphas, ICRF tails, and neutral beam populations. The collision operator consists both of the Monte Carlo equivalent Coulomb and an RF quasilinear diffusion collision operator; the latter is used to model the evolution of ICRF driven tails. A variety of particle diagnostics are tracked, including escaping particle energy, lifetime, and pitch angle distributions, energy and particle loss rates through the outer magnetic surface, and loss patterns on the outer surface. Confinement of thermal particles can also be examined both through calculations of local diffusion coefficients and global energy and particle losses through the outer magnetic flux surface. DELTA5D can be either run in a mode where it calculates the distribution function, f, or its deviation from a Maxwellian $\delta f$. The latter has been used especially in particle-based calculations of bootstrap current. An example of such a calculation is given below in Figure's 7 and 8.

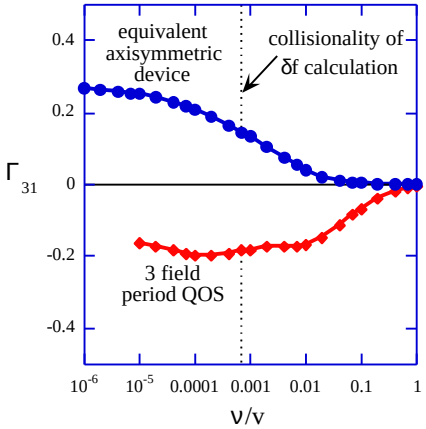


Figure 7 – $\Gamma_{31}$ transport coefficient vs. collisionality from DKES code for QOS and equivalent axisymmetric device

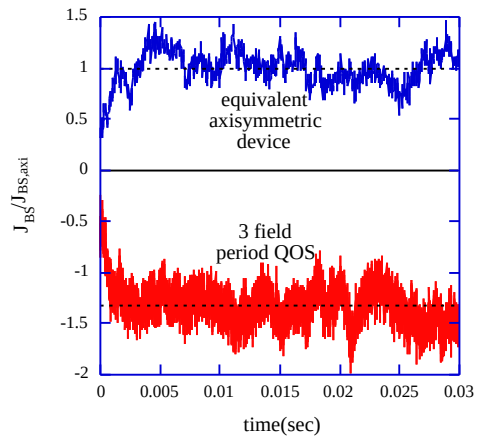


Figure 8 – Normalized bootstrap current for similar devices from δf particle code.

In the above Figures the transport coefficient, $\Gamma_{31}$ associated with bootstrap current is calculated using the DKES code as a function of collisionality (Figure 7) both for a three field period QOS device and its axisymmetric equivalent. In Figure 8 the bootstrap current based on the DELTA5D δf particle calculation (using 4096 particles) is shown at the collisionality indicated by the vertical dotted line in Figure 7. Both results show a reversal in bootstrap current for the non-axisymmetric QOS and roughly the same ratio of absolute magnitudes which occurs between the equivalent tokamak and the more helically dominated QOS device. Although the bootstrap currents in the two devices are similar in magnitude, the axisymmetric device would need substantial additional current to produce the assumed level of rotational transform whereas the QOS device needs no additional current (due to its shaping).

**Acknowledgements:** This research is sponsored by the Office of Fusion Energy U. S. Department of Energy, under contract DE-AC05-960R22464 with Lockheed Martin Energy Research Corp.

[1] S. P. Hirshman, D. A. Spong, J. C. Whitson, et al., Phys. Rev. Lett. Vol.80 1998 (528).

[2] D. A. Spong, S. P. Hirshman, J. C. Whitson, et al., Phys. Plasmas, Vol. 5 1998 (1752).

[3] D. A Spong, et al., IAEA-F1-CN-69/ICP/07, Proc. 17th IAEA Conf., Yokohama, Japan (1998).

[4] A. Reiman et al., IAEA-F1-CN-69/ICP/06, Proc. 17th IAEA Conf., Yokohama, Japan (1998).

[5] D. A. Spong, S. P. Hirshman, J. C. Whitson, IEEE Transactions on Plasma Science, Vol. 27, (Feb., 1999) 116; also, D. A. Spong, 16th Intl. Conf. On the Num. Simulation of Plasmas (1998) 39 (www.physics.ucla.edu/icnsp/Html/spong/spong.htm).

[6] U. Stroth et al., Nuclear Fusion **36**, 1063 (1996).

[7] W. Lotz, et al.,Plasma Phys. and Cont.r. Nuc. Fus. Res. (Proc. 13th Int. Conf., 1990) Vol. 3 IAEA, Vienna (1991) 525.

[8] D. Anderson, et al., Nuclear Fusion **6** (1994) 881.

[9] R. Sanchez, et al., submitted to J. Comp. Phys. (1999).

[10] W. I. Van Rij, S. P. Hirshman,, Phys. Fluids **B 1**, 563 (1989).